The American Mineralogist, Volume 60, pages 913–918, 1975

X-Ray Determination of Axially Symmetric Pole Fabrics from Interfering Reflections with Application to Orienting Mechanisms in Mica Aggregates

ROBERT J. TWISS[1] AND MICHAEL A. ETHERIDGE[2]

Research School of Earth Sciences, Australian National University, Canberra, A.C.T. 2600, Australia

Abstract

The X-ray texture goniometer is widely used to measure preferred orientations in polycrystalline materials. However, if the peak being measured overlaps or coincides with another reflection, the results may be erroneous. A method is presented here which corrects for the presence of the spurious reflection in axially symmetric fabrics, enabling determination of the true preferred orientation. The correction is applied to two sets of previously published data which give the preferred orientations of experimentally deformed mica aggregates. The uncorrected apparently contradictory results are found to be closely comparable after correction, supporting the conclusion in one of the papers that the orienting mechanism for micas is mechanical in cold strained samples and includes effects of crystallization in the hot strained samples.

Introduction

The X-ray texture goniometer is useful in measuring the fabric of a specific mineral plane $\{hkl\} = \{abc\}$ in a polycrystalline material. If the reflection peak from $\{abc\}$, however, closely overlaps peaks due to other crystallographic planes $\{hkl\} = \{\alpha\beta\gamma\}$, then the data need to be corrected before interpretation.

Such a situation may be encountered when measuring the preferred orientations of basal planes in mica. In some instruments, the *001* peak is unsuitable for such measurements because of excessive scattering of the beam at low 2θ values, and the *003* peak has to be used, with its immediately adjacent *022* reflection. For example, all of the preferred orientation results of Means and Paterson (1966) were determined from the *003* reflection with a beam divergence sufficient to include the whole *022* peak. This paper presents a correction procedure and applies it to the data of Means and Paterson (1966) to enable comparison with the closely related work of Etheridge, Paterson, and Hobbs (1974).

Correction Procedure

Assume the fabric of the poles to $\{abc\}$—here denoted $\perp \{abc\}$—is axially symmetric about **N** (Fig. 1). On the unit sphere, the goniometer inspects a band so as to detect reflections from those $\{abc\}$ whose poles lie in the band B_1. The band has a width Δl and its median line is defined in terms of the spherical polar coordinates (ϕ,ω) by $0 \leq \phi \leq \pi/2$ and $\omega = 0$, where $\phi = 0$ is defined to be the symmetry axis **N**.

Consider the small area A_1 in B_1 whose size is $(\Delta l)^2$ and whose center is at $(\phi,\omega) = (\Phi,0)$ where Φ is a particular value of the spherical polar coordinate ϕ. The total flux of X-rays $F_T^{A_1}$ from planes whose poles are in A_1 is the sum of $F_{abc}^{A_1}$ and $F_{\alpha\beta\gamma}^{A_1}$, the flux of reflections respectively from $\{abc\}$ and $\{\alpha\beta\gamma\}$. Thus

$$F_{abc}^{A_1} = F_T^{A_1} - F_{\alpha\beta\gamma}^{A_1} \qquad (1)$$

The analysis is easily extended to include more than the one interfering reflection considered here.

Crystals whose poles $\perp\{\alpha\beta\gamma\}$ lie in A_1 have their poles $\perp\{abc\}$ located somewhere in the small-circle band B_2 (Fig. 1). The width of this band is Δl. In the case that $\perp\{abc\}$ are not symmetrically distributed about $\perp(\alpha\beta\gamma)$ giving rise to more than one band like B_2, one of the bands, say the one with the smallest radius, may be specified.

Consider now an arbitrary area A_2 within B_2 having a size of $(\Delta l)^2$ (Fig. 1). All crystals with $\perp\{abc\}$ in A_2 will have $\perp\{\alpha\beta\gamma\}$ in a small-circle band B_3. This band has a width of Δl and necessarily includes the area A_1. If we assume no preferred orientation of $\perp\{\alpha\beta\gamma\}$ in B_3, then only a fraction of the crystals

[1] Now at: Department of Geology, University of California, Davis, California, 95616, U.S.A.

[2] Now at: Department of Earth Sciences, Monash University, Clayton, Victoria 3168, Australia.

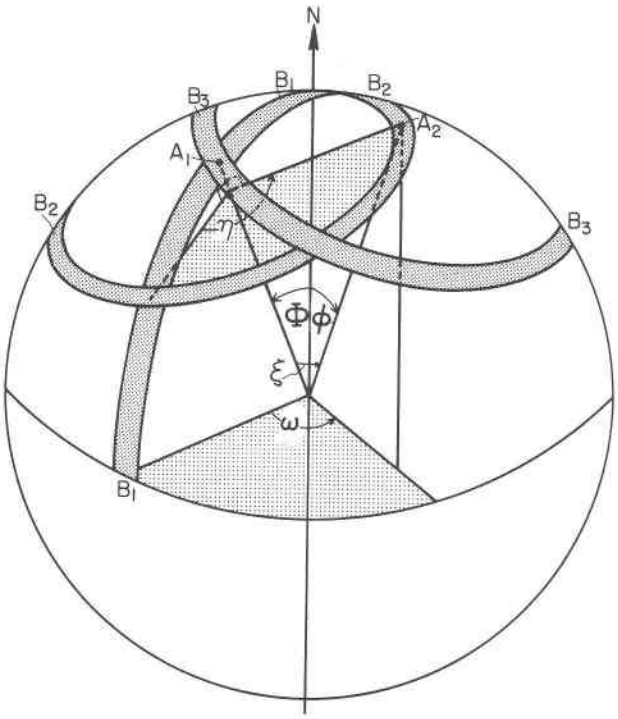

FIG. 1. Geometry for the correction procedure and the spherical polar coordinates used in the analysis.

with $\perp\{abc\}$ in A_2 will have their $\perp\{\alpha\beta\gamma\}$ in A_1. This fraction is given by the ratio of the areas of A_1 to B_3.

$$\frac{A_1}{B_3} = \frac{\Delta l \cdot \Delta l}{\Delta l \cdot C_3} = \frac{\Delta l}{C_3} \tag{2}$$

where C_3 is the circumference of B_3, and Δl is small.

For ease of analysis, we now introduce a second spherical polar coordinate system (ξ,η) centered with respect to the small-circle band B_2 (Fig. 1). The coordinate ξ is related to the first coordinate system such that $\xi = 0$ is the same line as $(\phi,\omega) = (\Phi,0)$. This line passes through the center of A_1. The coordinate η is measured in a plane normal to the line $\xi = 0$, and the point for which $\eta = 0$ is taken to lie on the mid-line of B_1. Thus the location of the area A_2, for example, can be specified in both coordinate systems by the respective coordinates (ϕ,ω) and (ξ,η) (Fig. 1). In this particular case the second coordinate system is set up so that ξ is the angle between $\perp\{abc\}$ and $\perp\{\alpha\beta\gamma\}$ and hence is the angle between the planes themselves.

Now at any point (μ,ρ) in spherical polar coordinates, define a function $I_{hkl}(\mu,\rho)$ having units of flux per unit length by

$$F^{A}_{hkl} \equiv I_{hkl}(\mu,\rho)\Delta l \tag{3}$$

Then those crystals with $\perp\{abc\}$ in A_2 will contribute to the flux $F^{A_1}_{\alpha\beta\gamma}$ by an amount given by

$$\delta F^{A_1}_{\alpha\beta\gamma} = \frac{A_1}{B_3}\int_{B_2} I_{\alpha\beta\gamma}(\xi,\eta)\, dC_3 = \frac{A_1}{B_3}(RF^{A_2}_{abc}) \tag{4}$$

where $R = (F_{\alpha\beta\gamma}/F_{abc})$ in a uniformly oriented aggregate.

Using Equations (3) and (4), then, the total flux due to $\perp\{\alpha\beta\gamma\}$ in A_1 is

$$F^{A_1}_{\alpha\beta\gamma} = \int_{B_2} \frac{\delta F^{A_1}_{\alpha\beta\gamma}}{\Delta l}\, dC_2$$

$$= R\frac{A_1}{B_3}\int_{B_2} I_{abc}(\xi,\eta)\, \mathrm{d}C_2 \tag{5}$$

where C_2 is the circumference of B_2.

Using Equations (2) and (3), and writing the integration explicitly gives

$$I_{\alpha\beta\gamma}(\Phi,0) = \frac{R}{C_3}\int_0^{2\pi} I_{abc}(\xi,\eta)\sin\xi\, d\eta$$

$$= \frac{2R}{C_3}\int_0^{\pi} I_{abc}(\xi,\eta)\sin\xi\, \mathrm{d}\eta \tag{6}$$

where $\mathrm{d}C_2 = \sin\xi\ \mathrm{d}\eta$. Now perform a coordinate transformation from (ξ,η) to (ϕ,ω) to obtain

$$I_{\alpha\beta\gamma}(\Phi,0) = \frac{2R}{C_3}\int_{|\Phi-\xi|}^{\Phi+\xi} I_{abc}(\phi,\omega)\sin\xi\frac{\partial\eta}{\partial\phi}\,\mathrm{d}\phi \tag{7}$$

where the lower limit of integration is taken as the absolute value because of the assumed symmetry of the fabric about **N**.

The two spherical polar coordinate systems are related by

$$\sin\xi\cos\eta = \cos\Phi\sin\phi\cos\omega - \sin\Phi\cos\phi \tag{8}$$

$$\sin\xi\sin\eta = \sin\phi\sin\omega \tag{9}$$

$$\cos\xi = \sin\Phi\sin\phi\cos\omega + \cos\Phi\cos\phi \tag{10}$$

From Equations (8) and (9)

$$\tan\eta = \frac{\sin\phi\sin\omega}{\cos\Phi\sin\phi\cos\omega - \sin\Phi\cos\phi} \tag{11}$$

From Equation (10)

$$\cos\omega = \frac{\cos\xi - \cos\Phi\cos\phi}{\sin\Phi\sin\phi} \tag{12}$$

$$[1-\cos^2\omega]^{1/2} = \sin\omega$$

$$= \frac{[\sin^2\Phi - \cos^2\xi - \cos^2\phi + 2\cos\Phi\cos\xi\cos\phi]^{1/2}}{\sin\Phi\sin\phi} \tag{13}$$

Now

$$\frac{\partial\tan\eta}{\partial\phi} = \frac{\partial\tan\eta}{\partial\eta}\frac{\partial\eta}{\partial\phi} = \frac{1}{\cos^2\eta}\frac{\partial\eta}{\partial\phi}$$

$$\frac{\partial\eta}{\partial\phi} = \cos^2\eta\frac{\partial\tan\eta}{\partial\phi} \tag{14}$$

Using Equations (12) and (13) to eliminate ω from Equations (8) and (11), and using the results in Equation (14), we obtain

$$\frac{\partial \eta}{\partial \phi} = \frac{\sin \phi}{[\sin^2 \Phi - \cos^2 \xi - \cos^2 \phi + 2 \cos \Phi \cos \xi \cos \phi]^{1/2}} \quad (15)$$

Using Equation (15) in Equation (7) gives

$$I_{\alpha\beta\gamma}(\Phi, 0) = \frac{2R}{C_3} \cdot \int_{|\Phi-\xi|}^{\Phi+\xi} \frac{I_{abc}(\phi,\omega) \sin\xi \sin\phi \mathrm{d}\phi}{[\sin^2 \Phi - \cos^2 \xi - \cos^2 \phi + 2 \cos \Phi \cos \xi \cos \phi]^{1/2}} \quad (16)$$

By dividing Equation (1) by Δl^2 and Equation (16) by Δl, the two equations may be combined to give the final form of the desired equation in units of flux per unit area (intensity)

$$\mathcal{I}_{abc}(\Phi, 0) = \mathcal{I}_T(\Phi, 0) - \frac{2R}{C_3} \cdot \int_{|\Phi-\xi|}^{\Phi+\xi} \frac{\mathcal{I}_{abc}(\phi, 0) \sin\xi \sin\phi \mathrm{d}\phi}{[\sin^2 \Phi - \cos^2 \xi - \cos^2 \phi + 2 \cos \Phi \cos \xi \cos \phi]^{1/2}} \quad (17)$$

where

$$\mathcal{I}_{hkl}(\Phi,0) = (1/\Delta l) I_{hkl}(\Phi,0) = (1/\Delta l^2) F^4_{hkl} \quad (18)$$

The solution of this equation may be approximated by breaking the integral into a summation over a finite number of intervals, and writing an equation for the intensity $\mathcal{I}_{abc}(\Phi,0)$ in each interval. The fabric has a plane of symmetry normal to the axis of symmetry **N**. Thus when $(\Phi + \xi) > 90°$, the summation may be written in terms of the intensity values between 0° and 90° only. If this quadrant is divided into $(n\text{-}1)$ intervals, we obtain a set of n simultaneous equations in n unknowns $\mathcal{I}_{abc}(\Phi_i)$, $(i = 1,2 \cdots, n)$.

Calculations in this paper were made for phlogopite with

$$\{abc\} = \{003\}$$
$$\{\alpha\beta\gamma\} = \{022\}$$
$$R = 0.4$$
$$\xi = 50°$$
$$n = 91$$

using a computer program written by R.J. Twiss. The value for R was obtained from Yoder and Eugster (1954); ξ equals (001) $\wedge$ (011) in phlogopite; the value for n gives intervals of one degree. While we did not check the approximation rigorously for convergence, empirically the behavior over the range $10 \leq n \leq 91$ indicated satisfactory solutions for the upper limit.

Application and Results

The problem of peak overlap when measuring mica basal plane preferred orientations from *003* reflections has been discussed briefly by Etheridge *et al* (1974). They stated that the errors could be removed either by modification of the X-ray instrument to eliminate scattered radiation at low 2θ values of the goniometer, or by the theoretical procedure outlined above. The instrument was accordingly modified, and the *001* reflection was used in all their measurements, but the theoretical correction was necessary for comparison with the apparently conflicting results which Means and Paterson (1966) obtained from similar experiments. We thus present corrected *003* data from both studies, and the measured *001* data from Etheridge *et al* (1974) in an attempt to resolve this conflict.

The measured X-ray intensity ($\mathcal{I}_M$) at $2\theta = 26.3°$ for the *003* peak for phlogopite (Yoder and Eugster, 1954) and a given value of Φ is:

$$\mathcal{I}_M(\Phi,0) = \mathcal{I}_{003}(\Phi,0) + \mathcal{I}_{022}(\Phi,0) + \mathcal{I}_B + \mathcal{I}_Q \quad (19)$$

where $\mathcal{I}_B$ is the background intensity extrapolated to the peak value, and $\mathcal{I}_Q$ is the intensity of diffracted X-rays from the overlapping quartz $10\bar{1}1$ peak (*cf* Etheridge *et al*, 1974, p.3). Both $\mathcal{I}_B$ and $\mathcal{I}_Q$ are assumed to be independent of Φ, and $\mathcal{I}_B$ can be measured; therefore $\mathcal{I}_B + \mathcal{I}_Q$ has a value which cannot exceed the lowest value on the measured intensity profile $\mathcal{I}_M$ $(\Phi,0)$. This value of $\mathcal{I}_M$ occurs at $(\Phi,0) = (\pi/2,0)$. Thus

$$\mathcal{I}_B + \mathcal{I}_Q \leq \mathcal{I}_M (\pi/2,0)$$
$$\mathcal{I}_Q \leq \mathcal{I}_M (\pi/2,0) - \mathcal{I}_B \equiv \mathcal{I}_X \quad (20)$$

Note that *before* solving Equation (17), the measured intensity values must be corrected for $\mathcal{I}_Q + \mathcal{I}_B$, *i.e.*,

$$\mathcal{I}_T = \mathcal{I}_M - (\mathcal{I}_Q + \mathcal{I}_B) = \mathcal{I}_X - \mathcal{I}_Q \quad (21)$$

The preferred orientation index (POI) is calculated for the corrected intensities using the following equation:

$$\mathrm{POI} = \frac{\mathcal{I}^{\max}_{003}}{\int_0^{\pi/2} \mathcal{I}_{003} \sin \Phi \, \mathrm{d}\Phi} \quad (22)$$

where $\mathcal{I}^{\max}_{003}$ is the maximum value of $\mathcal{I}_{003}(\Phi,0)$ which occurs at $\Phi = 0$ and where the integral in the denominator is approximated by a summation using $\mathcal{I}_{003}$ $(\Phi, 0)$ and ten degree steps in Φ.

TABLE 1. Theoretically Corrected Preferred Orientation Indices (POI) from Etheridge *et al** for Various Values of ϑ_Q

Run No.	T(°C) at Strain**	P.O.I. on (003)	Corrected P.O.I. for Listed Values of I_Q 0	$1/3I_X^\dagger$	$2/3I_X^\dagger$	$I_X^\dagger$	P.O.I. on (001)
748	25L	1.2	1.2	1.4	1.6	2.9	1.4
751	25L	1.2	1.2	1.3	1.5	2.8	1.2
759	25L	1.1	1.1	1.2	1.3	2.4	1.2
687	500C	1.5	1.7	1.9	2.5	5.1	2.3
689	500C	3.0	3.7	4.1	4.5	5.0	5.8
693	500C	1.8	2.0	2.3	3.0	4.1	3.0
694	500C	2.8	3.6	3.9	4.2	4.7	6.4
700	500C	2.6	3.1	3.4	4.0	4.8	3.4
735	500C	4.9	6.2	6.2	6.2	6.2	7.6
688	500L	1.5	1.7	1.9	2.5	4.0	2.5
691	500L	1.7	2.0	2.4	2.9	4.4	2.7
695	500L	3.0	3.9	4.2	4.6	5.0	7.1
701	500L	4.3	4.8	5.0	5.3	5.7	6.3
736	500L	4.9	6.4	6.4	6.4	6.4	7.0

*Etheridge *et al* (1974).
** *C* and *L* imply that straining occurred continuously and late respectively in the temperature cycle.
†$I_X = (I_M(\pi/2, 0) - I_B)$, *i.e.* I_X is the difference between the measured intensity at $\Phi=\pi/2$ and the background.

Changes in the POI from the theoretical correction arise essentially from two sources. First is the change introduced by different possible values of ϑ_Q; second is the change introduced by elimination of the interference from $\{\alpha\beta\gamma\}$ reflections.

For the first source, consider the simplified case for which $\vartheta_{\alpha\beta\gamma} = \vartheta_B = 0$. The intensity curves for ϑ_M and ϑ_T will then differ by the constant amount ϑ_Q (Eq. 21) which can be expressed (*cf* Eq. 20) as

$$\vartheta_Q = k\vartheta_X \quad 0 \leq k \leq 1 \tag{23}$$

Using the definition for the POI similar to Equation (22) and using Equation $(21)_1$ with Equation (23), we pose the problem

$$\text{POI (corrected)} \equiv \frac{\vartheta_T^{\max}}{A_T} \gtrless \frac{\vartheta_M^{\max}}{A_M}$$

$$= \frac{\vartheta_T^{\max} + k\vartheta_X}{A_T + A_D} \equiv \text{POI (uncorrected)}$$

where A_T and A_M are the total fluxes associated respectively with ϑ_T and ϑ_M through one half of the unit sphere, and A_D is the difference between these fluxes. A_D may thus be written

$$A_D = \int_0^{\pi/2} \vartheta_Q \sin\phi \, d\phi = k\vartheta_X \int_0^{\pi/2} \sin\phi \, d\phi = k\vartheta_X$$

Then because the POI is never less than one, it must hold that

$$\text{POI (corrected)} \equiv \frac{\vartheta_T^{\max}}{A_T}$$

$$\geq \frac{\vartheta_T^{\max} + k\vartheta_X}{A_T + kI_X} = \frac{\vartheta_M^{\max}}{A_M} \equiv \text{POI (uncorrected)}$$

A non-zero value of k will always result in a higher value for the corrected POI than the uncorrected POI. This is clearly seen in Tables 1 and 2 for $k = 0, 1/3, 2/3, 1$.

The changes in the POI accomplished by the theoretical correction for the $\{\alpha\beta\gamma\}$ reflections result from the different forms of the functions $\vartheta_{\alpha\beta\gamma}(\Phi)$ and $\vartheta_{abc}(\Phi)$. This is exemplified in Figure 2 for which $\vartheta_B = \vartheta_Q = 0$. The intensity distribution $\vartheta_{abc} = \vartheta_{003}$ was assumed, and the distributions for $\vartheta_{\alpha\beta\gamma} = \vartheta_{022}$ and $\vartheta_T = \vartheta_{003} + \vartheta_{022}$ were calculated from Equations (16) and (17). The maximum for ϑ_{022} is far removed from that for ϑ_{003} and ϑ_T has a broader distribution than ϑ_{003} because of the contribution of ϑ_{022}. Elimination of the ϑ_{022} component increases the POI from 4.6 to 6.8. The distribution of ϑ_{022}, of course, is intimately related to that of ϑ_{003} by the structure of the crystal. As a result, if ϑ_{003} is uniformly distributed, then so too will be ϑ_{022}, and we must conclude that the magnitude of the error (and hence the correction) in the POI due to interference from *022* will decrease with decreasing preferred orientation. This behavior is documented in Tables 1 and 2 and displayed in Figures 3 and 4.

Table 1 presents the results of a series of experiments in which the preferred orientation index was determined for both the *003* and the *001* reflections. The results of applying the theoretical correction to the POI on *003* for four values of ϑ_Q (for $k = 0,1/3,2/3,1$ in Eq. 23) are also presented in Table 1. The table indicates that the corrected POI's on *003* conform most nearly to the POI's on *001* for a value of $k = 2/3$.

Figure 3 shows graphically the relation between the POI on *003*, the preferred corrected POI on *003*, and the POI on *001*. At low to moderate POI's, the correc-

TABLE 2. Preferred Orientation Indices (POI) of Means and Paterson* and Theoretically Corrected POI for Various Values of ϑ_Q

Run No.	T(°C) at Strain**	Quoted P.O.I. on (003)	Corrected P.O.I. for Listed Values of I_Q 0	$1/3I_X^\dagger$	$2/3I_X^\dagger$	$I_X^\dagger$
198	25L	1.3	1.4	1.5	2.0	4.4
209	25L	1.3	1.4	1.6	2.0	3.4
260	25L	1.2	1.3	1.4	1.7	3.1
169	530E	1.8	1.9	2.2	2.7	3.7
199	530E	1.7	1.9	2.2	2.6	3.7
334	530E	2.8	3.4	3.8	4.2	4.9
174	600C	1.9	2.2	2.5	3.1	4.4
176	450C	1.5	1.7	1.9	2.5	4.2
168	530L	1.4	1.7	1.9	2.5	4.5
216	600L	1.2	1.2	1.3	1.5	3.3
331	530L	1.7	1.9	2.1	2.7	3.8

*Means and Paterson (1966).
**E, C, and L imply straining occurred early, continuously, and late, respectively, in the temperature cycle.
†$I_X = (I_M(\pi/2, 0) - I_B)$, *i.e.* I_X is the difference between the measured intensity at $\Phi=\pi/2$ and the background.

tion to the POI on *003* reproduces satisfactorily the POI on *001*. The correspondence is not as good at higher POI, but the correction is in the right direction and in general minimizes the change in the POI. The discrepancy may be accounted for at least in part by the fact that in samples having a high POI, the contribution to $\mathcal{I}_M$ $(\pi/2,0)$ from $\mathcal{I}_{003}$ and $\mathcal{I}_{022}$ is small, and even though the absolute amount of quartz present is small, $\mathcal{I}_Q$ will be a fraction (k) of $(\mathcal{I}_M(\pi/2,0)\text{-}\mathcal{I}_B)$ which approaches one. Thus the use of $k = 2/3$ to correct all POI's is a compromise which works least well for high values of the POI.

The most significant fact demonstrated by Figure 3, however, is that the correction with $k = 2/3$ successfully and accurately increases the distinction between the POI's for the cold- and the hot-strained samples.

Table 2 presents corrections for some of Means and Paterson's (1966) data selected to represent the range of their reported POI values. The data were taken from the original X-ray charts kindly provided by Dr. Paterson. Again four values of $\mathcal{I}_Q$ were used to produce a range of possible results.

Discussion

Means and Patterson (1966) concluded that the POI's on all of their specimens are indistinguishable, and that therefore the orienting mechanism for the platy minerals, which can be only mechanical rotation in the cold-strain experiments, must be the same for all their experimental conditions. Figure 4*a* presents the POI's determined from *003* reflections in phlogopite samples as reported in Means and Paterson (1966), Table 1. The lack of separation between their cold- and hot-strained samples seems to justify their conclusion. The results of our theoretical correction to the data, however, require a different conclusion.

Table 2 presents selected data from Means and Paterson's (1966) Table 1 along with the results of our theoretical corrections to those data. The most appropriate value of $\mathcal{I}_Q$ for accurately correcting low to moderate POI's appears to be $\mathcal{I}_Q = 2/3\mathcal{I}_X$. This is indicated by the experimental check on the correction discussed above and tabulated in Table 1.

Figures 4*b* and *c* are histograms plotted from Table 2 of the uncorrected POI's and the POI's corrected with $k = 2/3$. These figures show that the measured range of POI's of Means and Paterson (1.2 − 2.8) is significantly expanded (1.5 − 4.2), and the distinction between the cold- and hot-strained samples is significantly increased. Although statistical analysis of the

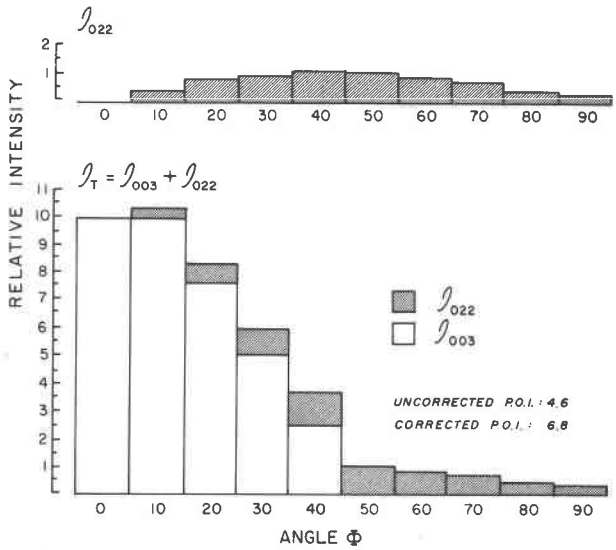

FIG. 2. Effect of interfering reflections on the true intensity distribution.

data in Figures 3 and 4 is not warranted, the interpretations given are consistent with the results of *t*-tests for the significance of the difference in mean values of the hot- and cold-strained samples using Equation 11.2.5 in Freund (1971).

Means and Paterson's runs 198, 209, and 260 (Table 2), which were heated first and then strained at 25°C, are all at the low end of the POI distribution, comparing closely with similarly deformed specimens of Etheridge *et al* (1974) (*e.g.*, 748, 751, 759, Table 1). Most of Means and Paterson's runs strained at high temperatures are at the high end of the distribution. These are very similar to comparably deformed specimens of Etheridge *et al* (1974) (Table 1).

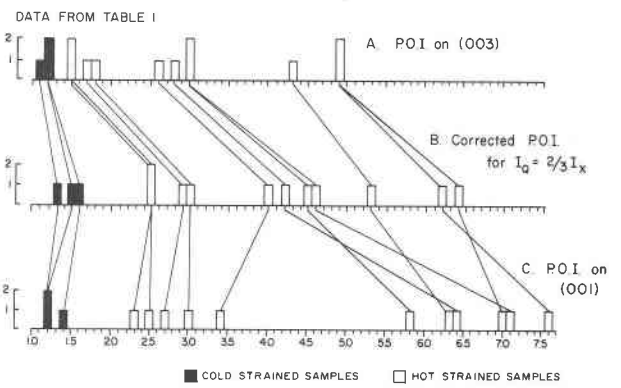

FIG. 3. Values of the preferred orientation index (POI) from Table 1. Lines between histograms connect values for the same sample A. POI determined on *003* reflections; B. POI from (A) after theorectical correction with $k = 2/3$; C. POI determined on *001* reflections.

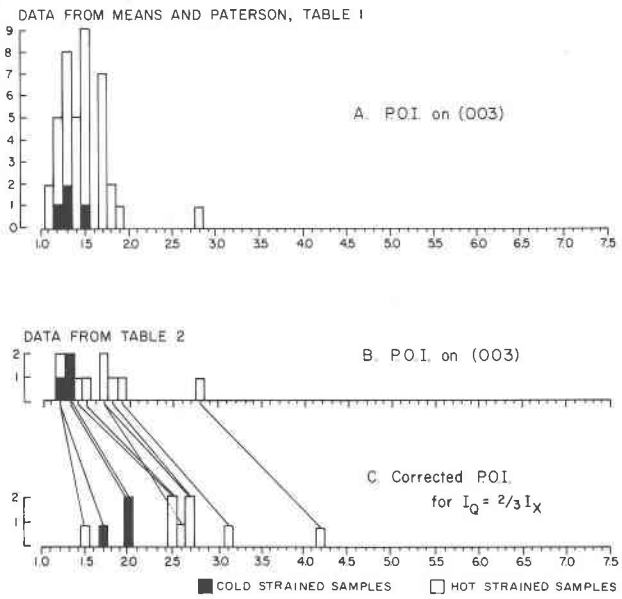

FIG. 4. Values of the preferred orientation index (POI). Lines between histograms connect values for the same sample. A. POI determined from *003* reflections as reported by Means and Paterson (1966), Table 1. B. POI selected from (a). See Table 2. C. POI from (b) after theoretical correction with $k = 2/3$. See Table 2.

It is thus concluded that there is a significant difference between the mica {001} preferred orientations of the hot (500°C) and cold (25°) strained specimens of Means and Paterson. These data appear to invalidate their conclusion about the orienting mechanism for the hot strained samples. Their corrected results are closely comparable with those of Etheridge *et al* (1974) and thus are consistent with the conclusions of the latter that although the low-temperature orienting process for phlogopite does indeed involve mechanical rotation, the high-temperature orienting processes involve the interaction of anisotropic growth rates with any or all of the following: anisotropic fluid movement, anisotropic pore structure, and the crystallographic anisotropy of "pressure solution."

Acknowledgments

We would like to thank B. E. Hobbs, G. S. Lister, and M. S. Paterson for comments and discussion throughout the work. W. D. Means first pointed out the possibility of interfering reflections in his X-ray measurements.

This work was done while Twiss held a NATO Postdoctoral Fellowship at the Australian National University. This support is gratefully acknowledged.

References

ETHERIDGE, M. A., M. S. PATERSON, AND B. E. HOBBS (1974) Experimentally produced preferred orientation in synthetic mica aggregates. *Contrib. Mineral. Petrol.* **44,** 275–294.

FREUND, JOHN E. (1971) *Mathematical Statistics,* Prentice-Hall, Inc., Englewood Cliffs, N.J., 463 p.

MEANS, W. D., AND M. S. PATERSON (1966) Experiments on preferred orientation of platy minerals. *Contrib. Mineral. Petrol.* **13,** 108–133.

YODER, H. S., AND H. P. EUGSTER (1954) Phlogopite synthesis and stability range. *Geochim. Cosmochim. Acta,* **6,** 157–185.

Manuscript received, November 1, 1974, accepted for publication, May 5, 1975.